Centrality Dependence of Charm Production from a Measurement of Single Electrons in Au + Au Collisions at $\sqrt{s_{NN}} = 200$ GeV

S. S. Adler,[5] S. Afanasiev,[17] C. Aidala,[5] N. N. Ajitanand,[43] Y. Akiba,[20,38] J. Alexander,[43] R. Amirikas,[12] L. Aphecetche,[45] S. H. Aronson,[5] R. Averbeck,[44] T. C. Awes,[35] R. Azmoun,[44] V. Babintsev,[15] A. Baldisseri,[10] K. N. Barish,[6] P. D. Barnes,[27] B. Bassalleck,[33] S. Bathe,[30] S. Batsouli,[9] V. Baublis,[37] A. Bazilevsky,[39,15] S. Belikov,[16,15] Y. Berdnikov,[40] S. Bhagavatula,[16] J. G. Boissevain,[27] H. Borel,[10] S. Borenstein,[25] M. L. Brooks,[27] D. S. Brown,[34] N. Bruner,[33] D. Bucher,[30] H. Buesching,[30] V. Bumazhnov,[15] G. Bunce,[5,39] J. M. Burward-Hoy,[26,44] S. Butsyk,[44] X. Camard,[45] J.-S. Chai,[18] P. Chand,[4] W. C. Chang,[2] S. Chernichenko,[15] C. Y. Chi,[9] J. Chiba,[20] M. Chiu,[9] I. J. Choi,[52] J. Choi,[19] R. K. Choudhury,[4] T. Chujo,[5] V. Cianciolo,[35] Y. Cobigo,[10] B. A. Cole,[9] P. Constantin,[16] D. G. d'Enterria,[45] G. David,[5] H. Delagrange,[45] A. Denisov,[15] A. Deshpande,[39] E. J. Desmond,[5] A. Devismes,[44] O. Dietzsch,[41] O. Drapier,[25] A. Drees,[44] R. du Rietz,[29] A. Durum,[15] D. Dutta,[4] Y. V. Efremenko,[35] K. El Chenawi,[49] A. Enokizono,[14] H. En'yo,[38,39] S. Esumi,[48] L. Ewell,[5] D. E. Fields,[33,39] F. Fleuret,[25] S. L. Fokin,[23] B. D. Fox,[39] Z. Fraenkel,[51] J. E. Frantz,[9] A. Franz,[5] A. D. Frawley,[12] S.-Y. Fung,[6] S. Garpman,[29,*] T. K. Ghosh,[49] A. Glenn,[46] G. Gogiberidze,[46] M. Gonin,[25] J. Gosset,[10] Y. Goto,[39] R. Granier de Cassagnac,[25] N. Grau,[16] S. V. Greene,[49] M. Grosse Perdekamp,[39] W. Guryn,[5] H.-Å. Gustafsson,[29] T. Hachiya,[14] J. S. Haggerty,[5] H. Hamagaki,[8] A. G. Hansen,[27] E. P. Hartouni,[26] M. Harvey,[5] R. Hayano,[8] N. Hayashi,[38] X. He,[13] M. Heffner,[26] T. K. Hemmick,[44] J. M. Heuser,[44] M. Hibino,[50] J. C. Hill,[16] W. Holzmann,[43] K. Homma,[14] B. Hong,[22] A. Hoover,[34] T. Ichihara,[38,39] V. V. Ikonnikov,[23] K. Imai,[24,38] D. Isenhower,[1] M. Ishihara,[38] M. Issah,[43] A. Isupov,[17] B. V. Jacak,[44] W. Y. Jang,[22] Y. Jeong,[19] J. Jia,[44] O. Jinnouchi,[38] B. M. Johnson,[5] S. C. Johnson,[26] K. S. Joo,[31] D. Jouan,[36] S. Kametani,[8,50] N. Kamihara,[47,38] J. H. Kang,[52] S. S. Kapoor,[4] K. Katou,[50] S. Kelly,[9] B. Khachaturov,[51] A. Khanzadeev,[37] J. Kikuchi,[50] D. H. Kim,[31] D. J. Kim,[52] D. W. Kim,[19] E. Kim,[42] G.-B. Kim,[25] H. J. Kim,[52] E. Kistenev,[5] A. Kiyomichi,[48] K. Kiyoyama,[32] C. Klein-Boesing,[30] H. Kobayashi,[38,39] L. Kochenda,[37] V. Kochetkov,[15] D. Koehler,[33] T. Kohama,[14] M. Kopytine,[44] D. Kotchetkov,[6] A. Kozlov,[51] P. J. Kroon,[5] C. H. Kuberg,[1,27] K. Kurita,[39] Y. Kuroki,[48] M. J. Kweon,[22] Y. Kwon,[52] G. S. Kyle,[34] R. Lacey,[43] V. Ladygin,[17] J. G. Lajoie,[16] A. Lebedev,[16,23] S. Leckey,[44] D. M. Lee,[27] S. Lee,[19] M. J. Leitch,[27] X. H. Li,[6] H. Lim,[42] A. Litvinenko,[17] M. X. Liu,[27] Y. Liu,[36] C. F. Maguire,[49] Y. I. Makdisi,[5] A. Malakhov,[17] V. I. Manko,[23] Y. Mao,[7,38] G. Martinez,[45] M. D. Marx,[44] H. Masui,[48] F. Matathias,[44] T. Matsumoto,[8,50] P. L. McGaughey,[27] E. Melnikov,[15] F. Messer,[44] Y. Miake,[48] J. Milan,[43] T. E. Miller,[49] A. Milov,[44,51] S. Mioduszewski,[5] R. E. Mischke,[27] G. C. Mishra,[13] J. T. Mitchell,[5] A. K. Mohanty,[4] D. P. Morrison,[5] J. M. Moss,[27] F. Mühlbacher,[44] D. Mukhopadhyay,[51] M. Muniruzzaman,[6] J. Murata,[38,39] S. Nagamiya,[20] J. L. Nagle,[9] T. Nakamura,[14] B. K. Nandi,[6] M. Nara,[48] J. Newby,[46] P. Nilsson,[29] A. S. Nyanin,[23] J. Nystrand,[29] E. O'Brien,[5] C. A. Ogilvie,[16] H. Ohnishi,[5,38] I. D. Ojha,[49,3] K. Okada,[38] M. Ono,[48] V. Onuchin,[15] A. Oskarsson,[29] I. Otterlund,[29] K. Oyama,[8] K. Ozawa,[8] D. Pal,[51] A. P. T. Palounek,[27] V. S. Pantuev,[44] V. Papavassiliou,[34] J. Park,[42] A. Parmar,[33] S. F. Pate,[34] T. Peitzmann,[30] J.-C. Peng,[27] V. Peresedov,[17] C. Pinkenburg,[5] R. P. Pisani,[5] F. Plasil,[35] M. L. Purschke,[5] A. K. Purwar,[44] J. Rak,[16] I. Ravinovich,[51] K. F. Read,[35,46] M. Reuter,[44] K. Reygers,[30] V. Riabov,[37,40] Y. Riabov,[37] G. Roche,[28] A. Romana,[25] M. Rosati,[16] P. Rosnet,[28] S. S. Ryu,[52] M. E. Sadler,[1] N. Saito,[38,39] T. Sakaguchi,[8,50] M. Sakai,[32] S. Sakai,[48] V. Samsonov,[37] L. Sanfratello,[33] R. Santo,[30] H. D. Sato,[24,38] S. Sato,[5,48] S. Sawada,[20] Y. Schutz,[45] V. Semenov,[15] R. Seto,[6] M. R. Shaw,[1,27] T. K. Shea,[5] T.-A. Shibata,[47,38] K. Shigaki,[14,20] T. Shiina,[27] C. L. Silva,[41] D. Silvermyr,[27,29] K. S. Sim,[22] C. P. Singh,[3] V. Singh,[3] M. Sivertz,[5] A. Soldatov,[15] R. A. Soltz,[26] W. E. Sondheim,[27] S. P. Sorensen,[46] I. V. Sourikova,[5] F. Staley,[10] P. W. Stankus,[35] E. Stenlund,[29] M. Stepanov,[34] A. Ster,[21] S. P. Stoll,[5] T. Sugitate,[14] J. P. Sullivan,[27] E. M. Takagui,[41] A. Taketani,[38,39] M. Tamai,[50] K. H. Tanaka,[20] Y. Tanaka,[32] K. Tanida,[38] M. J. Tannenbaum,[5] P. Tarján,[11] J. D. Tepe,[1,27] T. L. Thomas,[33] J. Tojo,[24,38] H. Torii,[24,38] R. S. Towell,[1] I. Tserruya,[51] H. Tsuruoka,[48] S. K. Tuli,[3] H. Tydesjö,[29] N. Tyurin,[15] H. W. van Hecke,[27] J. Velkovska,[5,44] M. Velkovsky,[44] V. Veszprémi,[11] L. Villatte,[46] A. A. Vinogradov,[23] M. A. Volkov,[23] E. Vznuzdaev,[37] X. R. Wang,[13] Y. Watanabe,[38,39] S. N. White,[5] F. K. Wohn,[16] C. L. Woody,[5] W. Xie,[6] Y. Yang,[7] A. Yanovich,[15] S. Yokkaichi,[38,39] G. R. Young,[35] I. E. Yushmanov,[23] W. A. Zajc,[9,†] C. Zhang,[9] S. Zhou,[7] S. J. Zhou,[51] and L. Zolin[17]

(PHENIX Collaboration)

[1]*Abilene Christian University, Abilene, Texas 79699, USA*
[2]*Institute of Physics, Academia Sinica, Taipei 11529, Taiwan*
[3]*Department of Physics, Banaras Hindu University, Varanasi 221005, India*

[4]Bhabha Atomic Research Centre, Bombay 400 085, India
[5]Brookhaven National Laboratory, Upton, New York 11973-5000, USA
[6]University of California at Riverside, Riverside, California 92521, USA
[7]China Institute of Atomic Energy (CIAE), Beijing, People's Republic of China
[8]Center for Nuclear Study, Graduate School of Science, University of Tokyo, 7-3-1 Hongo, Bunkyo, Tokyo 113-0033, Japan
[9]Columbia University, New York, New York 10027, USA
and Nevis Laboratories, Irvington, New York 10533, USA
[10]Dapnia, CEA Saclay, F-91191, Gif-sur-Yvette, France
[11]Debrecen University, H-4010 Debrecen, Egyetem tér 1, Hungary
[12]Florida State University, Tallahassee, Florida 32306, USA
[13]Georgia State University, Atlanta, Georgia 30303, USA
[14]Hiroshima University, Kagamiyama, Higashi-Hiroshima 739-8526, Japan
[15]Institute for High Energy Physics (IHEP), Protvino, Russia
[16]Iowa State University, Ames, Iowa 50011, USA
[17]Joint Institute for Nuclear Research, 141980 Dubna, Moscow Region, Russia
[18]KAERI, Cyclotron Application Laboratory, Seoul, Korea
[19]Kangnung National University, Kangnung 210-702, Korea
[20]KEK, High Energy Accelerator Research Organization, Tsukuba-shi, Ibaraki-ken 305-0801, Japan
[21]KFKI Research Institute for Particle and Nuclear Physics (RMKI), H-1525 Budapest 114, P.O. Box 49, Hungary
[22]Korea University, Seoul, 136-701, Korea
[23]Russian Research Center "Kurchatov Institute," Moscow, Russia
[24]Kyoto University, Kyoto 606, Japan
[25]Laboratoire Leprince-Ringuet, Ecole Polytechnique, CNRS-IN2P3, Route de Saclay, F-91128, Palaiseau, France
[26]Lawrence Livermore National Laboratory, Livermore, California 94550, USA
[27]Los Alamos National Laboratory, Los Alamos, New Mexico 87545, USA
[28]LPC, Université Blaise Pascal, CNRS-IN2P3, Clermont-Fd, 63177 Aubiere CEDEX, France
[29]Department of Physics, Lund University, Box 118, SE-221 00 Lund, Sweden
[30]Institut für Kernphysik, University of Muenster, D-48149 Muenster, Germany
[31]Myongji University, Yongin, Kyonggido 449-728, Korea
[32]Nagasaki Institute of Applied Science, Nagasaki-shi, Nagasaki 851-0193, Japan
[33]University of New Mexico, Albuquerque, New Mexico 87131, USA
[34]New Mexico State University, Las Cruces, New Mexico 88003, USA
[35]Oak Ridge National Laboratory, Oak Ridge, Tennessee 37831, USA
[36]IPN-Orsay, Universite Paris Sud, CNRS-IN2P3, BP 1, F-91406, Orsay, France
[37]PNPI, Petersburg Nuclear Physics Institute, Gatchina, Russia
[38]RIKEN (The Institute of Physical and Chemical Research), Wako, Saitama 351-0198, Japan
[39]RIKEN BNL Research Center, Brookhaven National Laboratory, Upton, New York 11973-5000, USA
[40]St. Petersburg State Technical University, St. Petersburg, Russia
[41]Universidade de São Paulo, Instituto de Física, Caixa Postal 66318, São Paulo CEP05315-970, Brazil
[42]System Electronics Laboratory, Seoul National University, Seoul, Korea
[43]Chemistry Department, Stony Brook University, SUNY, Stony Brook, New York 11794-3400, USA
[44]Department of Physics and Astronomy, Stony Brook University, SUNY, Stony Brook, New York 11794, USA
[45]SUBATECH (Ecole des Mines de Nantes, CNRS-IN2P3, Université de Nantes) BP 20722-44307, Nantes, France
[46]University of Tennessee, Knoxville, Tennessee 37996, USA
[47]Department of Physics, Tokyo Institute of Technology, Tokyo 152-8551, Japan
[48]Institute of Physics, University of Tsukuba, Tsukuba, Ibaraki 305, Japan
[49]Vanderbilt University, Nashville, Tennessee 37235, USA
[50]Waseda University, Advanced Research Institute for Science and Engineering, 17 Kikui-cho, Shinjuku-ku, Tokyo 162-0044, Japan
[51]Weizmann Institute, Rehovot 76100, Israel
[52]Yonsei University, IPAP, Seoul 120-749, Korea

(Received 28 September 2004; published 2 March 2005)

The PHENIX experiment has measured midrapidity transverse momentum spectra ($0.4 < p_T < 4.0$ GeV/c) of single electrons as a function of centrality in Au + Au collisions at $\sqrt{s_{NN}} = 200$ GeV. Contributions from photon conversions and Dalitz decays of light neutral mesons are measured by introducing a thin (1.7% X_0) converter into the PHENIX acceptance and are statistically removed. The subtracted nonphotonic electron spectra are primarily due to the semileptonic decays of hadrons containing heavy quarks, mainly charm at lower p_T. For all centralities, the charm production cross section is found to scale with the nuclear overlap function, T_{AA}. For minimum-bias collisions the charm cross section per binary collision is $N_{c\bar{c}}/T_{AA} = 622 \pm 57(\text{stat}) \pm 160(\text{syst})$ μb.

DOI: 10.1103/PhysRevLett.94.082301 PACS numbers: 25.75.Dw

In central Au + Au collisions at $\sqrt{s_{NN}} = 200$ GeV neutral pions and charged hadrons are strongly suppressed at high transverse momentum (p_T) [1–3]. In contrast, a modest high-p_T enhancement is observed in d + Au collisions at the same energy [4,5]. Taken together, these observations indicate that the suppression in Au + Au collisions is caused by final-state effects (e.g., parton energy loss in a dense medium produced in the reaction).

Heavy quarks (charm and bottom) are complementary probes of the hot and dense matter produced in high energy heavy ion collisions. Because of their large masses, charm and bottom cross sections are calculable via perturbative quantum chromodynamics (pQCD) and their yield is sensitive to the initial gluon density [6]. It has been predicted that heavy quarks suffer less energy loss than light quarks while traversing partonic matter due to the ''dead cone'' effect [7–9]. This can be studied through systematic measurements of the p_T spectra of open heavy flavor. In addition, the open-charm yield is an important baseline for understanding J/ψ production which has been predicted to be either suppressed [10] or enhanced [11] in deconfined partonic matter.

The PHENIX experiment observed that inclusive single electrons in central and minimum-bias Au + Au collisions at $\sqrt{s_{NN}} = 130$ GeV were produced in excess of purely ''photonic'' contributions (primarily due to π^0 Dalitz decays and conversion of π^0 photons in the detector material) [12]. This excess is consistent with the expected charm production, assuming that it scales with the number of binary nucleon-nucleon collisions ($N_{\rm coll}$) or, equivalently, with the nuclear overlap function, T_{AA}. In this Letter, we present results on the single electron measurement in $\sqrt{s_{NN}} = 200$ GeV Au + Au collisions. Our measurement is in a p_T range sensitive only to charm production. The new data have higher statistics and smaller systematic errors than the 130 GeV data, allowing us to measure charm production as a function of collision centrality.

The data used in this analysis were collected by the PHENIX detector [13] during the 2001 run period of the Relativistic Heavy Ion Collider. A coincidence of the beam-beam counters (BBC), a pair of detector arrays covering 2π in azimuth and $\eta = \pm(3.0$–$3.9)$, and the zero degree calorimeters (ZDC) provides the minimum-bias trigger ($92.2^{+2.5}_{-3.0}\%$ of the 6.8 ± 0.5 barn Au + Au inelastic cross section). The centrality is determined by the correlation between the multiplicity measured by the BBC and the energy of spectator neutrons measured by the ZDC. The BBC also measures the collision vertex, z, with resolution $\sigma = 0.7$ cm. We require $|z| < 20$ cm to eliminate electrons originating from the central magnet.

Charged particles are measured by the PHENIX east-arm spectrometer ($|\eta| < 0.35$, $\Delta\phi = \pi/2$) with resolution $\sigma_p/p \simeq 0.7\% \oplus 1.0\% p({\rm GeV}/c)$. Tracks are reconstructed with the drift chamber and the first layer of pad chambers and confirmed by requiring an electromagnetic calorimeter (EMCal) matching hit within 2σ in position. Electron candidates are required to have at least three associated hits in the ring imaging Čerenkov detector (RICH) that pass a ring shape cut, and are required to pass a timing cut in either the EMCal or the time-of-flight detector. After these cuts, a clear electron signal is observed as a narrow peak at $E/p = 1$. By requiring $-2\sigma < (E - p)/p < 3\sigma$, background from hadrons, which deposit only a fraction of their energy in the EMCal, and nonvertex electrons, which have misreconstructed momenta, is further reduced. Remaining background in the electron sample, due to accidental coincidences between RICH hits and hadron tracks, is estimated ($\approx 10\%$) and subtracted by an event-mixing method.

Inclusive electrons contain two components: (i) ''nonphotonic''—primarily semileptonic decays of mesons containing heavy quarks, and (ii) photonic—Dalitz decays of light neutral mesons (π^0, η, η', ρ, ω, and ϕ) and photon conversions in the detector material. To separate these two components, a photon converter (a thin brass tube of 1.7% radiation length surrounding the beam pipe at $r = 29$ cm) was installed.

We analyzed 2.2 M (2.5 M) events with the converter in (out). The corresponding raw electron p_T spectra for minimum-bias collisions are shown in Fig. 1(a). The photon converter multiplies the photonic contribution to the electron yield by a factor R_γ:

$$N_e^{\text{Conv-out}} = N_e^{\gamma} + N_e^{\text{non-}\gamma}, \tag{1}$$

$$N_e^{\text{Conv-in}} = R_\gamma N_e^{\gamma} + (1 - \epsilon) N_e^{\text{non-}\gamma}. \tag{2}$$

Here $N_e^{\text{Conv-in}}$ ($N_e^{\text{Conv-out}}$) is the measured electron yield with (without) the converter; N_e^{γ} ($N_e^{\text{non-}\gamma}$) is the electron yield due to the photonic (nonphotonic) component; and $\epsilon(\approx 2.1\%)$ represents a small loss of electrons due to the converter. We next define R_{CN} as the ratio of the raw electron yield with and without the converter. Dividing Eq. (2) by Eq. (1) and defining $R_{NP} \equiv N_e^{\text{non-}\gamma}/N_e^{\gamma}$, one has

$$R_{CN} \equiv \frac{N_e^{\text{Conv-in}}}{N_e^{\text{Conv-out}}} = \frac{R_\gamma + (1 - \epsilon) R_{NP}}{1 + R_{NP}}. \tag{3}$$

If there were no contribution from the nonphotonic component ($R_{NP} = 0$), then $R_{CN} = R_\gamma$.

The photonic electron yield per photon is approximately given by $Y \propto \delta + \frac{7}{9} t$, where δ is the Dalitz branching ratio per γ relative to 2γ (for π^0, η, and η') or 1γ (for ρ, ω, and ϕ) decay, and t is the thickness of the conversion material in radiation length (X_0). The factor $\frac{7}{9}$ is the approximate probability for a γ to convert in one X_0. Plugging in $\delta^{\pi^0} = 0.6\%$, $t \approx 1.1\%$ ($t \approx 2.8\%$) for converter out (in) we find $R_\gamma^{\pi^0} = Y^{\text{Conv-in}}/Y^{\text{Conv-out}} \approx 1.9$. There is some p_T depen-

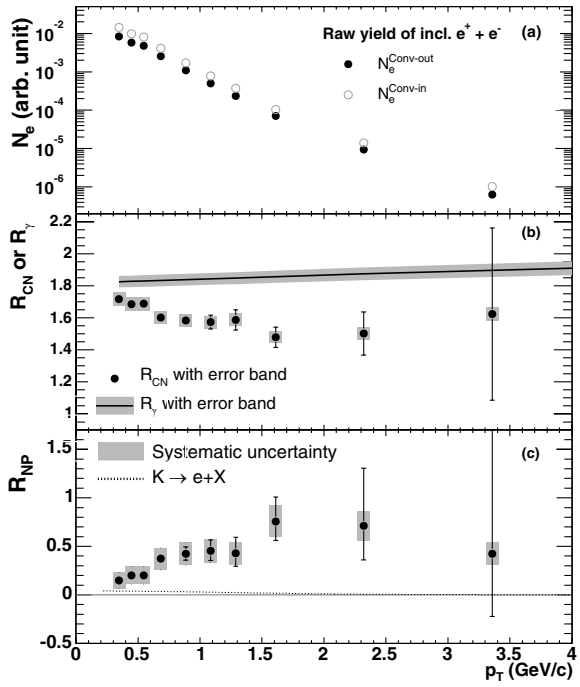

FIG. 1. Shown vs p_T (a) raw $e^{\pm}$ spectra measured with the converter in (open circles) and out (closed circles). (b) Ratio of the converter in/out $e^{\pm}$ yields (R_{CN}, points) and ratio of photonic $e^{\pm}$ yield with/without the converter (R_γ, line and shaded band). (c) Ratio of nonphotonic to photonic $e^{\pm}$ yields (R_{NP}, points) and contribution from kaon decays (dashed line).

dence in the complete formula for Y and the value of δ is species dependent ($\delta^\eta \approx 0.8\%$), so we perform a full GEANT [14] simulation with and without the converter to calculate R_γ. We determine R_γ for π^0 and η separately. We use the π^0 spectrum measured by PHENIX [1] as the input for the π^0 simulation and assume m_T scaling ($p_T \rightarrow \sqrt{p_T^2 + M_\eta^2 - M_\pi^2}$, normalized at high p_T to $\eta/\pi^0 = 0.45 \pm 0.1$) to obtain the input for the η simulation. Contributions from other mesons which undergo Dalitz decay (η', ρ, ω, ϕ) are small (6% at $p_T = 3$ GeV/c, and smaller at lower p_T). Since they have $\delta \approx \delta^\eta$, we assign them $R_\gamma = R_\gamma^\eta$. When calculating the combined R_γ, we use the particle ratios at high p_T ($\eta'/\pi^0 = 0.25 \pm 0.13$, $\rho/\pi^0 = \omega/\pi^0 = 1 \pm 0.5$, $\phi/\pi^0 = 0.4 \pm 0.2$). The ϕ/π^0 ratio used here is consistent with our π^0 and ϕ measurement [15]. The uncertainties in the particle ratios are included in the systematic uncertainties of R_γ. For this method it is essential that the amount of material is accurately modeled in the simulation. We compared the yield of identified photon conversion pairs in the data and in the simulation and conclude that the simulation reproduces R_γ within $\pm 2.0\%$. This uncertainty is included in the overall systematic uncertainty.

Figure 1(b) shows that R_{CN} gradually decreases with increasing p_T, while R_γ slightly increases with p_T. The difference between R_{CN} and R_γ indicates the existence of nonphotonic electrons. Figure 1(c) shows R_{NP} obtained from R_γ and R_{CN} using Eq. (3). R_{NP} increases with p_T and is more than 30% for $p_T > 0.6$ GeV/c. The small amount of conversion material in the PHENIX detector allows a sensitive measurement of R_{CN}.

Background from kaon decays ($K \rightarrow \pi e \nu$) and dielectron decays of ρ, ω, and ϕ remain in the nonphotonic electron yield. The background from kaon decays is estimated with a GEANT simulation using the kaon p_T spectrum measured by PHENIX [16] as input. The contribution of kaon decays to the nonphotonic yield, shown in Fig. 1(c), is 18% at $p_T = 0.4$ GeV/c and decreases rapidly to less than 6% for $p_T > 1$ GeV/c. To calculate background from the e^+e^- decays of ρ, ω, and ϕ, we first generate spectra by applying m_T scaling to the PHENIX π^0 spectrum, as described above. The contribution of these decays to the nonphotonic electrons is $<3\%$ for all p_T. Background from $J/\psi \rightarrow e^+e^-$ decays and from Drell-Yan pairs is negligible. Possible enhancement of low mass dileptons through $\pi + \pi \rightarrow \rho \rightarrow e^+e^-$, as reported in Pb + Pb collisions at the Super Proton Synchrotron [17], would contribute to the nonphotonic electrons. However, this is neglected since the estimated ρ contribution in the absence of enhancement is only $\approx 0.6\%$ over all p_T.

After these backgrounds are subtracted the only other significant source of nonphotonic electrons is the semileptonic decay of heavy flavor, overwhelmingly charm. We denote the remaining electrons as charm electrons. The raw spectrum of charm electrons is corrected for geometrical acceptance ($\epsilon_{\rm geo}$), track reconstruction efficiency ($\epsilon_{\rm rec}$), and electron identification efficiency ($\epsilon_{e\rm ID}$) determined by GEANT simulation. The efficiency $\epsilon_{\rm geo} \times \epsilon_{\rm rec}$ is about 11% of dN_e/dy, and $\epsilon_{e\rm ID}$ is about 65% as confirmed with electrons identified through photon conversion. Correction of multiplicity dependent efficiency losses, estimated by embedding simulated electron tracks into real events, is p_T independent and increases from 5% to 26% from peripheral to central collisions. The 1σ systematic uncertainty of these corrections is 11.8%. Fully corrected charm electron spectra are shown in Fig. 2 for minimum-bias collisions and for five centrality bins. We determined photonic electron spectra and found them to be in good agreement with the background calculated from the measured π^0 spectra using the method described in [12].

We also measured the charm electron spectrum in $p + p$ collisions at $\sqrt{s_{NN}} = 200$ GeV [18]. The lines in Fig. 2 show the best fit curve of this spectrum, scaled by T_{AA} for each Au + Au centrality bin. Here, T_{AA} is the nuclear overlap function calculated by a Glauber model [1] (Table I). The Au + Au data points are in reasonable agreement with the $p + p$ fit in all centrality bins.

To quantify the centrality dependence of charm production, we calculated the integrated yield dN_e/dy ($0.8 < p_T < 4.0$ GeV/c) and fit it to $AN_{\rm coll}^\alpha$, where A is constant. In the absence of medium effects $\alpha = 1$ is the expectation

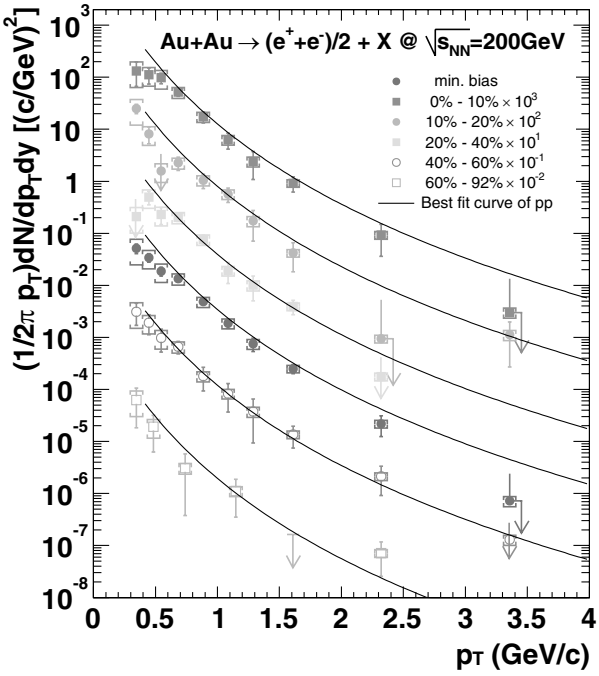

FIG. 2. Fully corrected charm electron p_T spectra for different Au + Au centralities scaled by successive factors of 10 for clarity. Error bars (brackets) correspond to statistical (systematic) uncertainties. Curves are described in the text.

in the absence of medium effects. In this comparison, most of the systematic effects will cancel. Figure 3 shows $dN_e/dy(0.8 < p_T < 4.0)/N_{\rm coll}$ vs $N_{\rm coll}$ for minimum bias and five centrality bins in Au + Au collisions and $p + p$ collisions. We find $\alpha = 0.938 \pm 0.075(\text{stat}) \pm 0.018(\text{syst})$. If $p + p$ data are included, $\alpha = 0.958 \pm 0.035(\text{stat})$. This shows that the total yield of charm electrons for all centralities is consistent with $N_{\rm coll}$ scaling.

For each centrality bin we scale the charm electron spectrum ($p_T > 0.8$ GeV/c) by T_{AA} and fit it with a PYTHIA calculation of the electron spectrum resulting from leading order charm and bottom production. We used PYTHIA 6.205 with a modified set of parameters (described in [12]) and CTEQ5L parton distribution functions [19]. Based on experimental input [20,21] we modified the PYTHIA default charm ratios, using instead $D^+/D^0 = 0.45 \pm 0.1$, $D_s/D^0 = 0.25 \pm 0.1$, and $\Lambda_c/D^0 = 0.1 \pm 0.05$.

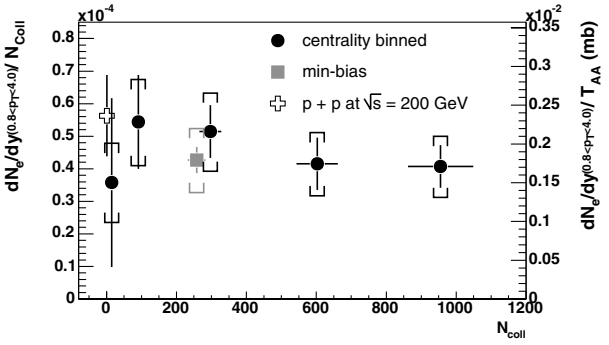

FIG. 3. Charm electron yield ($0.8 < p_T < 4.0$ GeV/c) measured in Au + Au collisions at 200 GeV scaled by $N_{\rm coll}$ as a function of $N_{\rm coll}$ (left-hand scale). Normalizing instead by the nuclear overlap function we obtain charm electron cross section per $N + N$ collision (right-hand scale).

This gives a $c \to e$ total branching ratio of $9.5 \pm 0.4\%$. Charmed hadron ratios from the statistical model [22] gives a similar branching ratio (9.3%). The scaled charm and bottom cross sections are treated as fit parameters, although our data are restricted to p_T values which are sensitive only to charm production. We evaluated the systematic error due to background subtraction ($\approx 21\%$) by refitting to the electron spectrum at the minimum and maximum of its 1σ systematic error band. The change of the p_T range for fitting the charm electron spectrum gives 3% systematic error for minimum-bias collisions. The systematic error due to the PYTHIA spectral shape ($\approx 11\%$) is dominated by the uncertainty in $\langle k_T \rangle = 1.5 \pm 0.5\,\text{GeV}/c$. Different parton distribution functions yield a systematic error of 6.2% for the rapidity-integrated cross section. These systematic errors are added in quadrature to give the overall systematic error on the charm cross section. For minimum-bias collisions we obtain $\frac{1}{T_{AA}} \frac{dN_{c\bar{c}}}{dy}|_{y=0} = 143 \pm 13(\text{stat}) \pm 36(\text{syst})\,\mu\text{b}$ and $N_{c\bar{c}}/T_{AA} = 622 \pm 57(\text{stat}) \pm 160(\text{syst})\,\mu\text{b}$. Results for all centrality bins are shown in Table I. The STAR collaboration reports a somewhat larger charm cross section ($\sigma_{c\bar{c}}^{NN} = 1.3 \pm 0.2 \pm 0.4 mb$) in $p + p$ and d + Au collision at $\sqrt{s_{NN}} = 200$ GeV [23]. Next-to leading order pQCD calculations of the charm production cross section have large associated uncertainties, with typical values between 300 and 450 μb [24].

TABLE I. Centrality bin, number of NN collisions, nuclear overlap function, charm cross section per NN collision, and total charm multiplicity per NN collision, in $\sqrt{s_{NN}} = 200$ GeV Au + Au reactions.

Centrality (%)	N_{coll}	T_{AA} (mb^{-1})	$\frac{1}{T_{AA}} \frac{dN_{c\bar{c}}}{dy}|_{y=0}$ (μb)	$N_{c\bar{c}}/T_{AA}$ (μb)
Minimum bias	258 ± 25	6.14 ± 0.45	143 ± 13 ± 36	622 ± 57 ± 160
0–10	955 ± 94	22.8 ± 1.6	137 ± 21 ± 35	597 ± 93 ± 156
10–20	603 ± 59	14.4 ± 1.0	137 ± 26 ± 35	596 ± 115 ± 158
20–40	297 ± 31	7.07 ± 0.58	168 ± 27 ± 45	731 ± 117 ± 199
40–60	91 ± 12	2.16 ± 0.26	193 ± 47 ± 52	841 ± 205 ± 232
60–92	14.5 ± 4.0	0.35 ± 0.10	116 ± 87 ± 43	504 ± 378 ± 190

We note that final-state effects influence only the momentum distribution of charm; they have little or no effect on the total open-charm yield. Therefore, our results indicate $N_{\rm coll}$ scaling of the initial charm production, as expected for pointlike pQCD processes. pQCD calculations without charm quark energy loss and hydrodynamic calculations assuming complete thermalization of charm quarks predict very similar charm electron spectra for $p_T < 2$ GeV/c [25]. Differentiating between these opposite physical pictures is possible only for $p_T > 2.5$ GeV/c, where statistics of the current analysis are limited.

In conclusion, we have measured single electrons from charm decays in Au + Au collisions at $\sqrt{s_{NN}} = 200$ GeV. We observe that the centrality dependence of charm quark production is consistent with $N_{\rm coll}$ scaling, as expected for hard processes. The much larger Au + Au data set collected by PHENIX in the 2003-04 run will allow us more detailed exploration of medium effects on charm production, both through deviations of the charm electron spectrum from $N_{\rm coll}$ scaling, and also through a measurement of charm quark flow.

We thank the staff of the Collider-Accelerator and Physics Departments at BNL for their vital contributions. We acknowledge support from the Department of Energy and NSF (USA), MEXT and JSPS (Japan), CNPq and FAPESP (Brazil), NSFC (China), CNRS-IN2P3 and CEA (France), BMBF, DAAD, and AvH (Germany), OTKA (Hungary), DAE and DST (India), ISF (Israel), KRF and CHEP (Korea), RMIST, RAS, and RMAE (Russia), VR and KAW (Sweden), U.S. CRDF for the FSU, U.S.-Hungarian NSF-OTKA-MTA, and U.S.-Israel BSF.

*Deceased.
†PHENIX Spokesperson.
Electronic address: zajc@nevis.columbia.edu

[1] S. S. Adler *et al.*, Phys. Rev. Lett. **91**, 072301 (2003).
[2] J. Adams *et al.*, Phys. Rev. Lett. **91**, 172302 (2003).
[3] S. S. Adler *et al.*, Phys. Rev. C **69**, 034910 (2004).
[4] S. S. Adler *et al.*, Phys. Rev. Lett. **91**, 072303 (2003).
[5] J. Adams *et al.*, Phys. Rev. Lett. **91**, 072304 (2003).
[6] J. A. Appel, Annu. Rev. Nucl. Part. Sci. **42**, 367 (1992).
[7] Y. L. Dokshitzer and D. E. Kharzeev, Phys. Lett. B **519**, 199 (2001).
[8] M. Djordjevic and M. Gyulassy, Phys. Lett. B **560**, 37 (2003).
[9] B. W. Zhang, E. Wang, and X.-N. Wang, Phys. Rev. Lett. **93**, 072301 (2004).
[10] T. Matsui and H. Satz, Phys. Lett. B **178**, 416 (1986).
[11] R. L. Thews, M. Schroedter, and J. Rafelski, Phys. Rev. C **63**, 054905 (2001).
[12] K. Adcox *et al.*, Phys. Rev. Lett. **88**, 192303 (2002).
[13] K. Adcox *et al.*, Nucl. Instrum. Methods Phys. Res., Sect. A **499**, 469 (2003).
[14] GEANT 3.2.1, CERN program library.
[15] R. Seto *et al.*, J. Phys. G **30**, S1017 (2004).
[16] S. S. Adler *et al.*, Phys. Rev. C **69**, 034909 (2004).
[17] G. Agakichiev *et al.*, Phys. Lett. B **422**, 405 (1998).
[18] S. Kelly *et al.*, J. Phys. G **30**, S1189 (2004).
[19] H. L. Lai *et al.*, Eur. Phys. J. C **12**, 375 (2000).
[20] D. Acosta *et al.*, Phys. Rev. Lett. **91**, 241804 (2003).
[21] K. Hagiwara *et al.*, Phys. Rev. D **66**, 010001 (2002).
[22] A. Andronic *et al.*, Phys. Lett. B **571**, 36 (2003).
[23] J. Adams *et al.*, nucl-ex/0407006.
[24] R. Vogt, hep-ph/0203151.
[25] S. Batsouli *et al.*, Phys. Lett. B **557**, 26 (2003).